CHAPTER 2

AN INVESTIGATION ON STRAIN AND TEMPERATURE RATE-DEPENDENT THERMOELASTICITY AND ITS INFINITE SPEED BEHAVIOUR

2.1 Introduction[1]

Cylindrical structures, characterized by their geometric simplicity yet wide-ranging applications, are integral components across diverse engineering domains. The interplay between thermal and mechanical forces in these structures is a critical aspect that influences their performance, durability, and safety. The significance of understanding the thermomechanical response of cylindrical structures lies at the heart of designing and optimizing the systems that used in various industries such as in aerospace, energy manufacturing and transportation. Through systematic analysis, it seeks to contribute valuable insights into stress distribution, heat transfer characteristics, and structural stability, all of which are paramount for the optimal design and operation of engineering systems. As we delve into the complexities of these structures under thermal and mechanical loading, the implications for industries ranging from energy to transportation become increasingly evident. Cylindrical structures, such as rocket motor casings and propulsion systems, are prevalent in aerospace engineering. The study of thermo-

[1]The content of this chapter is published in ***Journal of Thermal Stresses***, 43.3 (2020):269-283.

mechanical response is crucial for ensuring the safety and stability of these structures under high-temperature conditions, as well as potential transient thermal events. Cylindrical pressure vessels and boiler tubes are exposed to high temperatures and pressure gradients in applications like power generation. Understanding the thermomechanical response is crucial for designing safe and efficient systems, preventing structural failure, and ensuring compliance with safety standards. Cylindrical structures, such as tubes and pipes, are fundamental components of heat exchangers. These structures play a critical role in facilitating the transfer of heat between fluids. Analyzing the thermomechanical response of these tubes is essential for ensuring that they can withstand the thermal stresses associated with varying temperatures and pressure differentials. The geometric properties of an elastic medium containing a cylindrical cavity are of great interest in the field of science and technology. The study of such geometries provides valuable insight into the behaviour of materials under various conditions.

Bahar and Hetnarski (1978; 1979) proposed a technique to address coupled thermoelastic problems by employing the state-space methodology. This involves reformulating the problem in terms of state-space variables, specifically the displacement, temperature, and their respective gradients. The study conducted by Erbay and Suhubi (1986) examined the propagation of longitudinal waves in an infinite circular cylinder composed of a generalized thermoelastic material. The researchers derived the dispersion relation under the condition of maintaining a constant surface temperature for the cylinder. Wadhawan (1973) conducted the analysis of the problem of a circular cylinder with a stress-free boundary under a thermal shock. The problem pertaining to an infinite plate had been previously examined by Kolyano and Semerak (1973), while its analogous scenario involving a plate with a circular cavity was investigated by Chandrasekharaiah (1980). The problem related to an unbounded solid cylinder having a circular cylindrical cavity was addressed in the works of Furukawa et al. (1989; 1990) and an short-time approximated solution were obtained for one-dimesional problem corresponding to LS

theory. Sherief (1988) effectively solved the problem pertaining to generalized thermoelastic theory through the implementation of the state-space methodology. Boundary-initiated axisymmetric waves in an annular cylinder whose stress-free boundary surfaces subjected to thermal shock have been studied by Sherief and Anwar (1988). The field equations were formulated in unified forms that incorporate the coupled, LS, and GL models of thermoelasticity. Misra et al. (1987) conducted a study to investigate the impacts of mechanical and thermal relaxations in a viscoelastic medium that is subjected to heating and contains a cylindrical hole.

Chandrasekharaiah (1987) and some other researchers (Dhaliwal and Rokne (1989); Ignaczak and Mr´ owka Matejewska (1990)) have found out the discontinuity in displacement field for the GL model which contradicts the continuum hypothesis. Recently Yu et al. (2018) has developed strain-rate dependent theory of thermoelasticity (MGL) by using generalized dissipation inequality. This model modifies GL model by considering strain rate term in constitutive equation. Also, it has been reported here that the displacement field is continuous for one dimensional isotropic elastic half-space subjected to thermal shock on the boundary surface. Quintanilla (2018) has analysed some qualitative results on MGL model by considering a functional defined on the solutions of the problem. Several interesting publications pertaining to this chapter may be found in the following references Mohamed et.al. (2021), Tayel et al. (2022; 2021), Sarkar and De (2020), Sarkar et al. (2020a) and so forth. The layout of the present chapter is structured as follows. The strain-temperature-rate dependent theory of thermoelasticity (MGL) is merged with two additional generalized thermoelasticity theories (GL and LS) by the use of unified governing equations. In order to solve the problem, we apply Laplace transform technique to governing equations. However, the wave-like feature is transient in the context of generalized thermoelasticity theories. Consequently, the inverse Laplace transform is performed using the short-time approximation approach, resulting in the derivation of explicit expressions for the displacement, temperature,

and stress fields. The point of discontinuity is identified and the solution of the field variables is analysed independently within the framework of three models (GL, LS and MGL). It is observed that the displacement field in the MGL model demonstrates continuity. However, the characteristic feature predicted by the MGL model differs significantly from that of GL and LS models. The analytical findings obtained from the MGL model indicate the occurence of an infinite speed of disturbance. We further, carry out the numerical inversion of the Laplace transform by using the approach proposed by Bellman et al. (1966). Subsequently, in the last part a comparative graphical analysis of the findings is presented.

2.2 Governing Equations

In the context of generalized thermoelasticity theories, the basic governing equations for the homogeneous, isotropic elastic body for the LS, GL, and MGL can be written in a unified way as follows (Lord and Shulman (1967); Green and Lindsay (1972); Yu et al. (2018)):

Stress-displacement relation in the absence of external body force:

$$\sigma_{ij,j} = \rho \frac{\partial^2 u_i}{\partial t^2} \tag{2.2.1}$$

Stress-strain temperature relation:

$$\sigma_{ij} = (1 + z_1 \tau_1 \frac{\partial}{\partial t})(2\mu e_{ij} + \lambda e_{kk} \delta_{ij}) - \gamma(\theta + z_2 \tau_1 \frac{\partial \theta}{\partial t})\delta_{ij} \tag{2.2.2}$$

Heat conduction equation in the absence of external heat source:

$$k\theta_{,ii} = \rho c_E (\frac{\partial \theta}{\partial t} + z_3 \tau_0 \frac{\partial^2 \theta}{\partial t^2}) + \gamma \theta_0 (\frac{\partial e_{ij}}{\partial t} + z_4 \tau_0 \frac{\partial^2 e_{ij}}{\partial t^2})\delta_{ij} \tag{2.2.3}$$

The linear strain-displacement relation:

$$e_{ij} = \frac{u_{i,j} + u_{j,i}}{2} \tag{2.2.4}$$

Based on different set of values of z_1, z_2, z_3 and z_4 we can obtain the equations in the context of different models as follows:

Case I: LS model: $z_1 = z_2 = 0$ and $z_3 = z_4 = 1$

Case II : GL model: $z_1 = z_4 = 0$ and $z_2 = z_3 = 1$

Case III : MGL model: $z_1 = z_2 = z_3 = z_4 = 1$.

On combining Eq. (2.2.1) and Eq. (2.2.2), we obtain

$$\rho\frac{\partial^2 u_i}{\partial t^2} = (1 + z_1\tau_1\frac{\partial}{\partial t})(2\mu e_{ij} + \lambda e_{kk}\delta_{ij})_{,j} - \gamma(\theta + z_2\tau_1\frac{\partial\theta}{\partial t})_{,j}\delta_{ij} \tag{2.2.5}$$

2.3 Formulation of the Problem

In this study, we examine an infinite isotropic elastic media containing a cylindrical cavity with a radius of a. The cavity is aligned in the z-direction and covers the area beyond $r > a$, as shown in Figure. It is assumed that there are no body forces or heat sources present, and the interior surface of the cavity is free from any external tractions. However, at time $t > 0$, the inner boundary of the cavity is instantaneously subjected to uniform heating and remains in that condition. In the present investigation, we use the assumption that the body exhibits symmetry around the z-axis. Consequently, the available data indicates that the displacement vector consists of a single component alone in the radial direction, denoted as $u(r, t)$. The stress tensor is characterised by two components, namely σ_{rr} and $\sigma_{\phi\phi}$, which correspond to the normal and transverse directions, respectively. Consequently, the radial strain and hoop strain may be expressed as :

$$e_{rr} = \frac{\partial u}{\partial r}, e_{\phi\phi} = \frac{u}{r}, \tag{2.3.1}$$

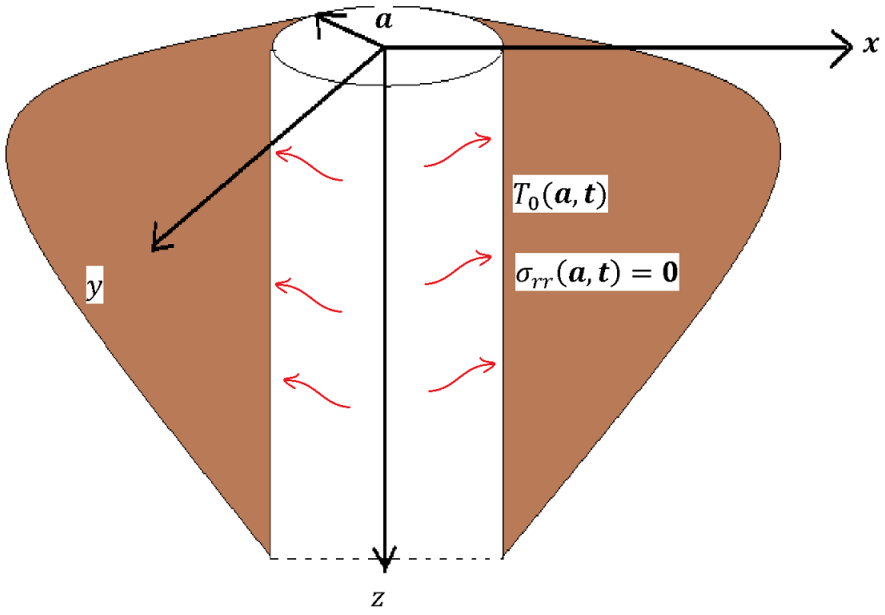

Figure 2.3.1: Geometry of elastic medium with a cylindrical cavity

The dilation e is given by

$$e = e_{kk} = \frac{\partial u}{\partial r} + \frac{u}{r} \tag{2.3.2}$$

Further, the equation of motion is given by

$$\frac{\partial \sigma_{rr}}{\partial r} + \frac{\sigma_{rr} - \sigma_{\phi\phi}}{r} = \rho \frac{\partial^2 u}{\partial t^2} \tag{2.3.3}$$

On combining Eqs. (2.2.5-2.3.2), we get

$$\rho \frac{\partial^2 u}{\partial t^2} = (2\mu + \lambda)(1 + z_1 \tau_1 \frac{\partial}{\partial t})(\frac{\partial^2 u}{\partial r^2} + \frac{1}{r}\frac{\partial u}{\partial r} - \frac{u}{r^2}) - \gamma(1 + z_2 \tau_1 \frac{\partial}{\partial t})\frac{\partial \theta}{\partial r} \tag{2.3.4}$$

Applying Eq. (2.3.1) and Eq. (2.3.2) in Eq. (2.2.3), we get

$$k\left(\frac{\partial^2 \theta}{\partial r^2} + \frac{1}{r}\frac{\partial \theta}{\partial r}\right) = \rho c_E(\frac{\partial \theta}{\partial t} + z_3 \tau_0 \frac{\partial^2 \theta}{\partial t^2}) + \gamma \theta_0 (1 + z_4 \tau_0 \frac{\partial}{\partial t})\frac{\partial e}{\partial t} \tag{2.3.5}$$

Further, the non-zero stress components are given by

$$\sigma_{rr} = (1 + z_1\tau_1\frac{\partial}{\partial t})\left[(2\mu + \lambda)\frac{\partial u}{\partial r} + \lambda\frac{u}{r}\right] - \gamma(1 + z_2\tau_1\frac{\partial}{\partial t})\theta \tag{2.3.6}$$

$$\sigma_{\phi\phi} = (1 + z_1\tau_1\frac{\partial}{\partial t})\left[(2\mu + \lambda)\frac{u}{r} + \lambda\frac{\partial u}{\partial r}\right] - \gamma(1 + z_2\tau_1\frac{\partial}{\partial t})\theta \tag{2.3.7}$$

In order to ease our calculation, we proceed to transform Eqs. (2.3.4-2.3.7) into dimensionless forms by employing the subsequent relationships:

$$(r^*, u^*) = c_0\eta\,(r, u)\,, (t^*, \tau_0^*, \tau_1^*) = c_0^2\eta\,(t, \tau_0, \tau_1)\,, \theta^* = \frac{\theta}{\theta_0}, \left(\sigma_{rr}^*, \sigma_{\phi\phi}^*\right) = \frac{(\sigma_{rr}, \sigma_{\phi\phi})}{(2\mu + \lambda)}, e^* = e \tag{2.3.8}$$

where

$$c_0^2 = \frac{(2\mu + \lambda)}{\rho}, \eta = \frac{\rho c_E}{k}$$

After omitting the superscript $(*)$ for the sake of simplicity, we derive the non-dimensional versions of Eqs. (2.3.4-2.3.7) as follows:

$$\frac{\partial^2 d}{\partial t^2} = (1 + z_1\tau_1\frac{\partial}{\partial t})(\frac{\partial^2 u}{\partial r^2} + \frac{1}{r}\frac{\partial u}{\partial r} - \frac{u}{r^2}) - a_1(1 + z_2\tau_1\frac{\partial}{\partial t})\frac{\partial\theta}{\partial r} \tag{2.3.9}$$

$$\left(\frac{\partial^2\theta}{\partial r^2} + \frac{1}{r}\frac{\partial\theta}{\partial r}\right) = (\frac{\partial\theta}{\partial t} + z_3\tau_0.\frac{\partial^2\theta}{\partial t^2}) + a_2(1 + z_4\tau_0\frac{\partial}{\partial t})\frac{\partial e}{\partial t} \tag{2.3.10}$$

$$\sigma_{rr} = (1 + z_1\tau_1\frac{\partial}{\partial t})\left[\frac{\partial u}{\partial r} + \lambda_1\frac{u}{r}\right] - a_1(1 + z_2\tau_1\frac{\partial}{\partial t})\theta \tag{2.3.11}$$

$$\sigma_{\phi\phi} = (1 + z_1\tau_1\frac{\partial}{\partial t})\left[\frac{u}{r} + \lambda_1\frac{\partial u}{\partial r}\right] - a_1(1 + z_2\tau_1\frac{\partial}{\partial t})\theta \tag{2.3.12}$$

whe re $a_1 = \frac{\gamma\Theta_0}{(2\mu+\lambda)}, a_2 = \frac{\gamma}{\eta k}, \lambda_1 = \frac{\lambda}{(2\mu+\lambda)}$.

Now we shall proceed with the assumption that the body under consideration is initially

held in an undeformed state, with its temperature denoted as θ_0. Furthermore, we shall consider the following set of initial conditions as being applicable:

For $t = 0$ and $r \geqslant a$ (dimensionless)

$$\theta(r,0) = \frac{\partial\theta}{\partial t}(r,0) = u(r,0) = \frac{\partial u}{\partial t}(r,0) = 0 \tag{2.3.13}$$

2.4 Boundary Conditions

We have taken into account the following inner boundary condition:

for $r = a$, and $t > 0$

$$\left.\begin{aligned} \sigma_{rr}(a,t) &= 0 \\ \theta(a,t) &= T_0 H(t) \end{aligned}\right\} \tag{2.4.1}$$

where $H(t)$ is the Heaviside unit function and T_0 is a constant temperature.

2.5 Formulation in Laplace Transform Domain

Taking the Laplace transform of Eqs. (2.3.9-2.3.12) with respect to time under the homogeneous initial conditions given by Eq. (2.3.13), we obtain

$$s^2\overline{u} = b_0\left(\frac{\partial^2\overline{u}}{\partial r^2} + \frac{1}{r}\frac{\partial\overline{u}}{\partial r} - \frac{\overline{u}}{r^2}\right) - a_1 b_1 \frac{\partial\overline{\theta}}{\partial r} \tag{2.5.1}$$

$$\left(\frac{\partial^2\overline{\theta}}{\partial r^2} + \frac{1}{r}\frac{\partial\overline{\theta}}{\partial r}\right) = b_2\overline{\theta} + a_2 b_3\overline{e} \tag{2.5.2}$$

$$\overline{\sigma}_{rr} = b_0\left[\frac{\partial\overline{u}}{\partial r} + \lambda_1\frac{\overline{u}}{r}\right) - a_1 b_1\overline{\theta} \tag{2.5.3}$$

$$\overline{\sigma}_{\phi\phi} = b_0\left[\frac{\overline{u}}{r} + \lambda_1\frac{\partial\overline{u}}{\partial r}\right) - a_1 b_1\overline{\theta} \tag{2.5.4}$$

where

$$b_0 = 1 + z_1\tau_1 s, b_1 = 1 + z_2\tau_1 s, b_2 = s\left(1 + z_3\tau_0 s\right), b_3 = s\left(1 + z_4\tau_0 s\right) \tag{2.5.5}$$

and s is the Laplace transform parameter.

Using the expression of e into Eq. (2.5.1) ,we get

$$s^2\overline{u} = b_0\frac{\partial\overline{e}}{\partial r} - a_1 b_1\frac{\partial\overline{\theta}}{\partial r} \tag{2.5.6}$$

On solving Eqs. (2.5.2) and (2.5.6), we obtain

$$b_0\nabla^4\overline{\theta} - \left(b_0 b_2 + \epsilon b_1 b_3 + s^2\right)\nabla^2\overline{\theta} + s^2 b_2\overline{\theta} = 0 \tag{2.5.7}$$

Similarly, we obtain

$$b_0\nabla^4\overline{e} - \left(b_0 b_2 + \epsilon b_1 b_3 + s^2\right)\nabla^2\overline{e} + s^2 b_2\overline{e} = 0 \tag{2.5.8}$$

where $\epsilon = a_1 a_2, \nabla^2 = \frac{\partial^2}{\partial r^2} + \frac{1}{r}\frac{\partial}{\partial r}$

Above equations can be written as

$$\left(\frac{\partial^2}{\partial r^2} + \frac{1}{r}\frac{\partial}{\partial r} - m_1^2\right)\left(\frac{\partial^2}{\partial r^2} + \frac{1}{r}\frac{\partial}{\partial r} - m_2^2\right)\overline{\theta} = 0 \tag{2.5.9}$$

$$\left(\frac{\partial^2}{\partial r^2} + \frac{1}{r}\frac{\partial}{\partial r} - m_1^2\right)\left(\frac{\partial^2}{\partial r^2} + \frac{1}{r}\frac{\partial}{\partial r} - m_2^2\right)\overline{e} = 0 \tag{2.5.10}$$

Here, n_1^2 and n_2^2 are the roots of the following characterstic equation:

$$n_1 x^4 - n_2 x^2 + n_3 = 0 \tag{2.5.11}$$

where $n_1 = b_0, n_2 = b_0 b_2 + \epsilon b_1 b_3 + s^2, n_3 = s^2 b_2$

The solutions of Eqs. (2.5.9) and (2.5.10) that are bounded at infinity can be written

as

$$\overline{\theta} = A_1 K_0 (m_1 r) + A_2 K_0 (m_2 r) \tag{2.5.12}$$

$$\overline{e} = B_1 K_0 (m_1 r) + B_2 K_0 (m_2 r) \tag{2.5.13}$$

where A_i and B_i are the arbitrary constants and $K_0 (m_i r)$ is the modified Bessel function of second kind of zero order. The constants A_i and B_i are not independent. By using Eqs. (2.5.12) and (2.5.13) into Eq. (2.5.2), we get a relation between A_i and B_i as

$$B_i = f_i A_i \tag{2.5.14}$$

where $f_i = \frac{\left(m_i^2 - b_2\right)}{a_2 b_3}$

Put the value of $\overline{\theta}$ and $\overline{e}$ from Eqs. (2.5.12) and (2.5.13) into Eqs. (2.5.1), (2.5.3) and (2.5.4) and we obtain $\overline{u}$, $\overline{\sigma}_{rr}$ and $\overline{\sigma}_{\phi\phi}$, respectively as

$$\overline{u} = \sum_{i=1}^{2} C_i A_i K_1 (m_i r) \tag{2.5.15}$$

$$\overline{\sigma}_{rr} = \sum_{i=1}^{2} A_i S_i^r \tag{2.5.16}$$

$$\overline{\sigma}_{\phi\phi} = \sum_{i=1}^{2} A_i S_i^{\phi} \tag{2.5.17}$$

where

$$C_i = \frac{\left(-b_0 f_i + a_1 b_1\right) m_i}{s^2} \tag{2.5.18}$$

$$S_i^r = \left[-C_i b_0 n_i - a_1 b_1\right] K_0\left(m_i r\right) + \frac{\left(\lambda_1 - 1\right) b_0}{r} C_i K_1\left(m_i r\right) \tag{2.5.19}$$

$$S_i^\phi = \left[-\lambda_1 C_i b_0 n_i - a_1 b_1\right] K_0\left(m_i r\right) + \frac{\left(1 - \lambda_1\right) b_0}{r} C_i K_1\left(m_i r\right) \tag{2.5.20}$$

Now, taking the Laplace transform of Eq. (2.4.1), we get

$$\overline{\sigma}_{rr}(a,t) = 0,$$

$$\overline{\Theta}(a,t) = \frac{T_0}{s}$$

Applying the above boundary condition in Eqs. (2.5.12) and 2.5.16), we get the values of $A_1$and A_2 as

$$A_1 = \frac{-S_2^a T_0}{s\left(S_1^a K_0\left(m_2 a\right) - S_2^a K_0\left(m_1 a\right)\right)} \tag{2.5.21}$$

$$A_2 = \frac{S_1^a T_0}{s\left(S_1^a K_0\left(m_2 a\right) - S_2^a K_0\left(m_1 a\right)\right)} \tag{2.5.22}$$

where

$$S_i^a = \left[-C_i b_0 m_i - a_1 b_1\right] K_0\left(m_i a\right) + \frac{\left(\lambda_1 - 1\right) b_0}{a} C_i K_1\left(m_i a\right) \tag{2.5.23}$$

Eqs. (2.5.12), (2.5.15-2.5.17) are the solution to the problem in the transformed domain (r, s).

2.6 Short-Time Approximated Solution

The solutions provided by Eqs. (2.5.12), (2.5.15-2.5.17) exhibit intricate function dependencies on the Laplace transform parameter, denoted as 's'. Consequently, the task

of determining the inverse Laplace transform to obtain a concise analytical solution for the problem becomes exceedingly challenging, if not practically unattainable. In this particular section, we have successfully derived an analytical solution for a short duration by employing the method of approximating the function using Maclaurin's series expansions and leaving aside the higher order terms of negligible magnitude. In the context of the Laplace transform, we make the assumption that the parameter 's' is significantly large. By utilising Maclaurin's series expansion and leaving aside higher order terms of $1/s$, we obtain the approximated roots, denoted as m_1 and m_2, for Eq. (2.5.11) in the MGL model.

$$m_1 \approx m_{11}s + m_{12} + \frac{m_{13}}{s}$$

$$m_2 \approx n_{21}\sqrt{s} + \frac{m_{22}}{\sqrt{s}} + \frac{m_{23}}{s^{\frac{3}{2}}}$$

where

$$m_{11} = \sqrt{p_1}, m_{12} = \frac{p_2}{2\sqrt{p_1}}, m_{13} = \frac{-p_2^2 + 4p_1p_3}{8p_1^{\frac{3}{2}}},$$

$$m_{21} = \sqrt{P_1}, m_{22} = \frac{P_2}{2\sqrt{P_1}}, m_{23} = \frac{-P_2^2 + 4P_1P_3}{8P_1^{\frac{3}{2}}},$$

$$p_1 = \frac{1}{2}\left(\sqrt{c_1} + \frac{M_1}{\tau_1}\right), p_2 = \frac{1}{2}\left(\frac{c_2}{2\sqrt{c_1}} + \frac{M_1N_1}{\tau_1}\right), p_3 = \frac{1}{2}\left(\frac{c_3}{2\sqrt{c_1}} + \frac{M_1N_2}{\tau_1} - \frac{c_2^2}{8c_1^{\frac{3}{2}}}\right),$$

$$P_1 = \frac{1}{2}\left(-\frac{c_2}{2\sqrt{c_1}} + \frac{M_1N_1}{\tau_1}\right), P_2 = \frac{1}{2}\left(-\frac{c_3}{2\sqrt{c_1}} + \frac{M_1N_2}{\tau_1} + \frac{c_2^2}{8c_1^{\frac{3}{2}}}\right),$$

$$P_3 = \frac{1}{2}\left(-\frac{c_4}{2\sqrt{c_1}} + \frac{M_1N_3}{\tau_1} + \frac{c_2c_3}{4c_1^{\frac{3}{2}}} - \frac{c_2^3}{16c_1^{\frac{5}{2}}}\right)$$

$$c_1 = \left(\frac{M_1}{\tau_1}\right)^2, c_2 = \left(\frac{M_1}{\tau_1}\right)^2 (2N_1) - 4\frac{\tau_0}{\tau_1}, c_3 = \left(\frac{M_1}{\tau_1}\right)^2 \left(2N_2 + N_1^2\right) + 4\left(\frac{\tau_0}{\tau_1^2} - \frac{1}{\tau_1}\right),$$

$$c_4 = \left(\frac{M_1}{\tau_1}\right)^2 (2N_2N_1 + 2N_3) + 4\left(\frac{1}{\tau_1^2} - \frac{\tau_0}{\tau_1^3}\right),$$

$$N_1 = \frac{1}{M_1}\left(M_2 - \frac{M_1}{\tau_1}\right), N_2 = \frac{1}{M_1}\left(M_3 - \frac{M_2}{\tau_1} + \frac{M_1}{\tau_1^2}\right), N_3 = \frac{1}{M_1}\left(-\frac{M_3}{\tau_1} + \frac{M_2}{\tau_1^2} - \frac{M_1}{\tau_1^3}\right),$$

$$M_1 = (1+\epsilon)\,\tau_0\tau_1, M_2 = (1+\epsilon)\,(\tau_0 + \tau_1) + 1, M_3 = (1+\epsilon)\,.$$

Now, by substituting the values of m_1 and m_2 from above equations into Eqs. (2.5.12), (2.5.15-2.5.17) and using the expressions

$$K_0(ax) \approx e^{-ax}\sqrt{\frac{\pi}{2x}}\left[\frac{1}{\sqrt{a}} - \frac{1}{8x\,(a)^{\frac{3}{2}}} + \frac{9}{128x^2\,(a)^{\frac{5}{2}}}\right]$$

$$K_1(ax) \approx e^{-ax}\sqrt{\frac{\pi}{2x}}\left[\frac{1}{\sqrt{a}} + \frac{3}{8x\,(a)^{\frac{3}{2}}} - \frac{15}{128x^2\,(a)^{\frac{5}{2}}}\right]$$

after detail manipulation, we obtain the solutions for the distributions of temperature, displacement and stresses in the Laplace domain (r, s) for large s as follows:

$$\overline{\theta} = \frac{\theta^*\sqrt{a}}{\sqrt{r}}\left[e^{-m_1(r-a)}\left(\frac{H_{21}}{s^2} + \frac{H_{22}}{s^{\frac{5}{2}}}\right) + e^{-m_2(r-a)}\left(\frac{H_{23}}{s} + \frac{H_{24}}{s^{\frac{3}{2}}}\right)\right] \tag{2.6.1}$$

$$\overline{u} = \frac{\theta^*\sqrt{a}}{\sqrt{r}}\left[e^{-m_1(r-a)}\left(\frac{h_{31}}{s^2} + \frac{h_{32}}{s^{\frac{5}{2}}}\right) + e^{-m_2(r-a)}\left(\frac{h_{34}}{s^{\frac{3}{2}}} + \frac{h_{35}}{s^2}\right)\right] \tag{2.6.2}$$

$$\overline{\sigma}_{rr} = \frac{\theta^*\sqrt{a}}{\sqrt{r}}\left[e^{-m_1(r-a)}\left(h_{41} + \frac{h_{42}}{s^{\frac{1}{2}}}\right) + e^{-m_2(r-a)}\left(h_{51} + \frac{h_{52}}{s^{\frac{1}{2}}}\right)\right] \tag{2.6.3}$$

$$\overline{\sigma}_{\phi\phi} = \frac{\theta^* \sqrt{a}}{\sqrt{r}} \left[e^{-m_1(r-a)} \left(H_{41} + \frac{H_{42}}{s^{\frac{1}{2}}} \right) + e^{-m_2(r-a)} \left(H_{51} + \frac{H_{52}}{s^{\frac{1}{2}}} \right) \right] \tag{2.6.4}$$

Taking the inverse Laplace transform of Eqs. (2.6.1-2.6.4) by using the formulae

$$L^{-1}\left(\frac{e^{\frac{-a}{s}}}{s^2} \right) = \left(\frac{t}{a} \right)^{\frac{1}{2}} J_1\left(2\sqrt{at} \right), a > 0$$

$$L^{-1}\left(\frac{e^{\frac{-a}{s}}}{s^{\frac{5}{2}}} \right) = \frac{sin\left(2\sqrt{at} \right)}{2\sqrt{\pi} a^{\frac{3}{2}}} - \frac{t^{\frac{1}{2}} cos\left(2\sqrt{at} \right)}{\sqrt{\pi} a}, a > 0$$

$$L^{-1}\left(\frac{e^{-a\sqrt{s}}}{s} \right) = erfc\left(\frac{a}{2\sqrt{t}} \right), a > 0$$

$$L^{-1}\left(\frac{e^{-a\sqrt{s}}}{s^{\frac{3}{2}}} \right) = \left(\frac{2\sqrt{t}}{\sqrt{\pi}} e^{\frac{-a^2}{4t}} - a * erfc\left(\frac{a}{2\sqrt{t}} \right) \right), a > 0$$

$$L^{-1}\left(\frac{e^{-a\sqrt{s}}}{s^2} \right) = \left(\left(t + \frac{a^2}{2} \right) erfc\left(\frac{a}{2\sqrt{t}} \right) - \frac{a\sqrt{t}}{\sqrt{\pi}} e^{-\frac{a^2}{4t}} \right), a > 0$$

We obtain the final short-time approximated solutions for the distributions of temperature, displacement and stresses in the physical domain (r, t) for MGL model as

$$\begin{aligned} \theta(r,t) = \theta_2 \Bigg[& e^{-m_{32}} H(t - r_1 m_{11}) \left(H_{21} \left(\frac{t - r_1 m_{11}}{m_{33}} \right)^{\frac{1}{2}} J_1\left(2\sqrt{m_{33}(t - r_1 m_{11})} \right) \right. \\ & \left. + H_{22} \left(\frac{sin\left(2\sqrt{m_{33}(t - r_1 m_{11})} \right)}{2\sqrt{\pi} m_{33}^{\frac{3}{2}}} - \frac{(t - r_1 m_{11})^{\frac{1}{2}} cos\left(2\sqrt{m_{33}(t - r_1 m_{11})} \right)}{\sqrt{\pi} m_{33}} \right) \right) \\ & + H_{23} erfc\left(\frac{m_{41}}{2\sqrt{t}} \right) + H_{24} \left(\frac{2\sqrt{t}}{\sqrt{\pi}} e^{\frac{-m_{41}^2}{4t}} - m_{41} erfc\left(\frac{m_{41}}{2\sqrt{t}} \right) \right) \Bigg] \end{aligned} \tag{2.6.5}$$

$$\begin{aligned} u(r,t) = \theta_2 \Bigg[& e^{-m_{32}} H(t - r_1 m_{11}) \left(h_{31} \left(\frac{t - r_1 m_{11}}{n_{33}} \right)^{\frac{1}{2}} J_1\left(2\sqrt{m_{33}(t - r_1 m_{11})} \right) \right. \\ & \left. + h_{32} \left(\frac{sin\left(2\sqrt{m_{33}(t - r_1 m_{11})} \right)}{2\sqrt{\pi} m_{33}^{\frac{3}{2}}} - \frac{(t - m_{31})^{\frac{1}{2}} cos\left(2\sqrt{m_{33}(t - r_1 m_{11})} \right)}{\sqrt{\pi} m_{33}} \right) \right) \\ & + h_{34} \left(\frac{2\sqrt{t}}{\sqrt{\pi}} e^{\frac{-m_{41}^2}{4t}} - m_{41} * erfc\left(\frac{m_{41}}{2\sqrt{t}} \right) \right) \\ & + h_{35} \left(\left(t + \frac{m_{41}^2}{2} \right) erfc\left(\frac{m_{41}}{2\sqrt{t}} \right) - \frac{m_{41}\sqrt{t}}{\sqrt{\pi}} e^{-\frac{m_{41}^2}{4t}} \right) \Bigg] \end{aligned} \tag{2.6.6}$$

$$\sigma_{rr} = \theta_2 \left[e^{-m_{32}} H(t - r_1 m_{11}) \left(h_{41} \left(\delta(t - r_1 m_{11}) - \frac{(m_{33})^{\frac{1}{2}} J_1 \left(2\sqrt{m_{33}(t - r_1 m_{11})} \right)}{(t - r_1 m_{11})^{\frac{1}{2}}} \right) + \frac{h_{42} cos \left(2\sqrt{m_{33}(t - r_1 m_{11})} \right)}{\sqrt{\pi}(t - r_1 m_{11})^{\frac{1}{2}}} \right) + h_{51} \frac{m_{41}}{2\sqrt{\pi}(t)^{\frac{3}{2}}} e^{\frac{-m_{41}^2}{4t}} + \frac{h_{52}}{\sqrt{\pi}(t)^{\frac{1}{2}}} e^{\frac{-m_{41}^2}{4t}} \right] \tag{2.6.7}$$

$$\sigma_{\phi\phi} = \theta_2 \left[e^{-m_{32}} H(t - r_1 m_{11}) \left(H_{41} \left(\delta(t - r_1 m_{11}) - \frac{(m_{33})^{\frac{1}{2}} J_1 \left(2\sqrt{m_{33}(t - r_1 m_{11})} \right)}{(t - r_1 m_{11})^{\frac{1}{2}}} \right) + \frac{H_{42} cos \left(2\sqrt{m_{33}(t - r_1 m_{11})} \right)}{\sqrt{\pi}(t - r_1 m_{11})^{\frac{1}{2}}} \right) + H_{51} \frac{m_{41}}{2\sqrt{\pi}(t)^{\frac{3}{2}}} e^{\frac{-m_{41}^2}{4t}} + \frac{H_{52}}{\sqrt{\pi}(t)^{\frac{1}{2}}} e^{\frac{-m_{41}^2}{4t}} \right] \tag{2.6.8}$$

where $erfc(x)$ is the complementary error function defined by

$$erfc(x) = \frac{2}{\sqrt{\pi}} \int_x^{\infty} e^{-t^2} dt,$$

$$\theta_2 = T_0 \sqrt{\frac{a}{r}},$$

and $r_1 = r - a, m_{31} = r_1 m_{11}, m_{32} = r_1 m_{12}, m_{33} = r_1 m_{13}, m_{41} = r_1 m_{21}$. The expressions of different notations (H_{ij},h_{ij}) used in above solutions are provided in Appendix I.

2.7 Analysis of Analytical Results

It is observed that the short-time approximation solutions for the field variables, as described by Eqs. (2.6.5-2.6.8), is a resultant of dual-term structure in the context of the MGL model. The first portion of the expression attached to the term $H(t - r_1 m_{11})$ represents a wave that is propagating at a velocity of $\frac{1}{m_{11}}$ in close proximity to the wave-front $r = a + \frac{t}{m_{11}}$. The first portion of the expressions provided by equations (2.6.5-2.6.8) indicates that the waves exhibit exponential decay, with an attenuating coefficient of m_{32}. It is readily apparent that the velocity and attenuation coefficient of waves are contingent upon both the material properties and the relaxation time.

The another component of the expressions shown in Eqs. (2.6.5-2.6.8) does not exhibit any contribution to the wave phenomenon. Instead, it displays diffusive characteristics, suggesting an infinite speed of disturbance. Moreover, it is worth noting that the temperature and displacement fields exhibit a continuous nature, while the stress components, on the other hand, encounter delta-function singularities precisely at the thermal wave-front.

According to Chandrasekharaiah (1992), in the context LS model when $z_1 = z_2 = 0$ and $z_3 = z_4 = 1$, it has been observed that the solution for each field is combination of two components. These components are characterised by wave types that propagate at a finite speed and exhibit exponential decay with respect to radial distance. Based on the findings presented, it has been demonstrated that displacement exhibits continuity. While, it is important to note here that the temperature and stress components experience discontinuity at both the elastic and thermal wave-fronts.

Chandrasekharaiah (1992) investigated that in the context of the GL model, namely when $z_1 = z_4 = 0$ and $z_2 = z_3 = 1$, the solution consists of two distinct parts. These portions correspond to wave types that propagate at a limited speed and exhibit exponential decay with the radial distance. In this specific case, it has been also revealed that displacement and temperature exhibit discontinuities, whereas stress components experience infinite discontinuities at the wave-fronts.

It can be inferred that the MGL model effectively addresses the issue of unrealistic prediction of discontinuity in the displacement field, which is exhibited in the GL model. Nevertheless, it is important to note that the solution for each field variable may be categorised into combination of two components: a wave component and a diffusive component. Furthermore, it has been shown that these waves propagate at an infinite speed, similar to what is seen in the visco-thermoelastic model. The observation that elastic waves can travel with unbounded speed suggests that, according to the current model, the influence of disturbances in the material are instantaneously felt throughout

the entire space. The observed behaviour of the solution in this modified GL model is found to be unrealistic, in contrast to the GL and LS model. The LS and GL model anticipate limited speeds for both elastic and thermal waves, leading to a restricted range of effect.

2.8 Numerical Results and Discussions

In this particular section, our objective is to determine the numerical solution of the physical fields within the framework of the MGL model. Subsequently, we will proceed to compare these obtained results with the corresponding outcomes derived from the generalized models, namely the GL and LS models. The numerical inversion method employed in this study is based on the work of Bellman et al. (1966). To implement this method, a Matlab-based algorithm is utilised. The selected material for the purpose of conducting the numerical evaluation is copper.

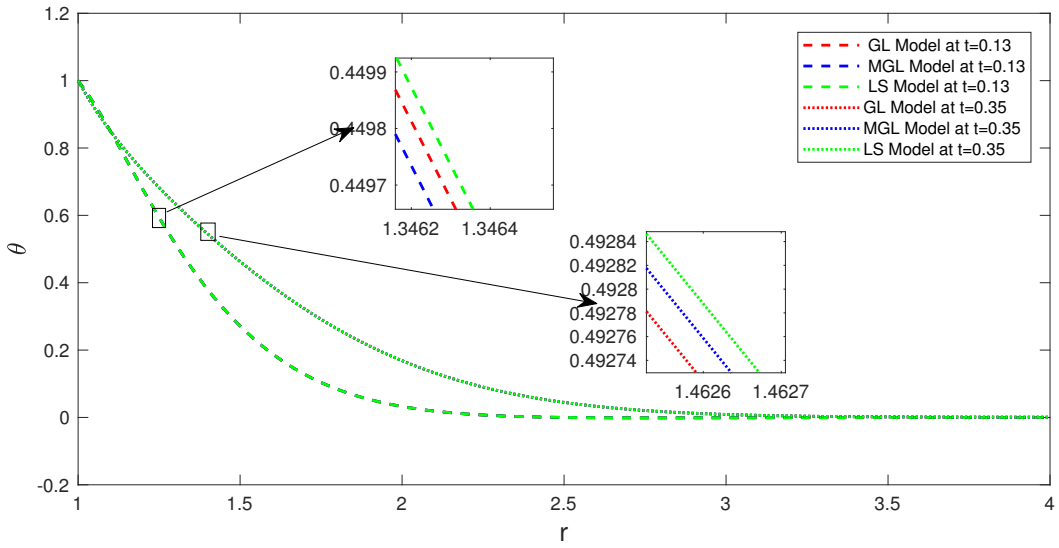

Figure 2.8.1: Variation of temperature for three models at time $t = 0.13$ and $t = 0.35$

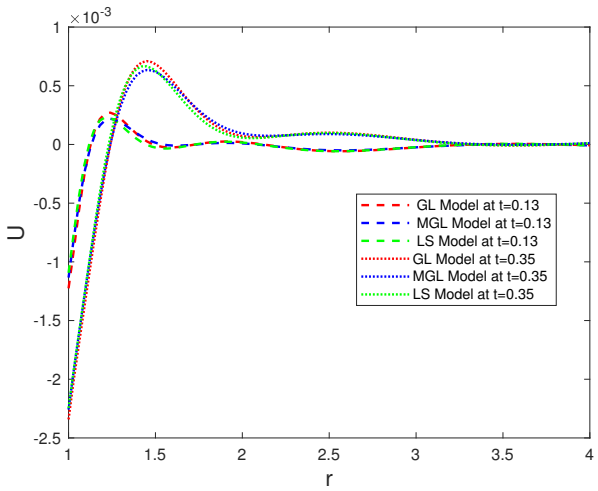

Figure 2.8.2: Variation of displacement for three models at time $t = 0.13$ and $t = 0.35$

The provided information includes the physical data for the mentioned material.

$$\lambda = 7.76 \times 10^{10}\,\mathrm{Nm}^{-2}, \mu = 3.86 \times 10^{10}\,\mathrm{Nm}^{-2}, \alpha = 1.78 \times 10^{-5}\mathrm{K}^{-1},$$

$$\eta = 8886.73\,\mathrm{sm}^{-2}, c_E = 383.1\,\mathrm{JKg}^{-1}\mathrm{K}^{-1}, \rho = 8954\,\mathrm{Kg\,m}^{-3}, T_0 = 293\,\mathrm{K}$$

We assume the hypothetical values of the dimensionless relaxation parameters as $\tau_0 = 0.01$ and $\tau_1 = 0.02$.

The field variables, including radial stress, hoop stress, temperature, and displacement, exhibit dependence on both time and radial distance, as well as on relaxation parameters denoted as τ_0 and τ_1. The numerical solutions for the field variables are computed directly using Eqs. (2.5.12) and (2.5.15-2.5.17), and are afterwards shown in various figures. In figures (2.8.1-2.8.4), the variation of dimensionless field values with respect to radial distance ($r > 1$) at two distinct time was graphically shown for the three models: GL, MGL, and LS.

In figure (2.8.1), it can be observed that there is no statistically significant variance in temperature values across the three models in relation to the radial distance, r.

Additionally, it is evident that temperature has the highest value at the inner boundary of cavity, and subsequently it declines rapidly as the radial distance increases.

Based on the analysis of figure (2.8.2), it is evident that a peak displacement is attained at a certain distance from the boundary. Furthermore, as time progresses, this maximum displacement is observed at increasingly larger radial distances. The observed trend in displacement is characterised by an initial negative value followed by a rapid increase towards positive values.

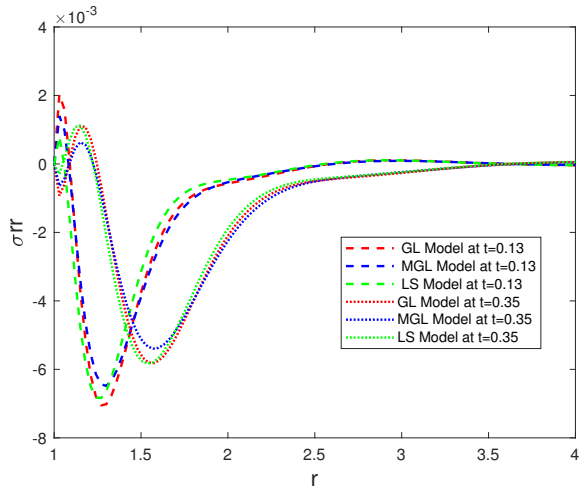

Figure 2.8.3: Variation of radial stress for three models at time $t = 0.13$ and $t = 0.35$

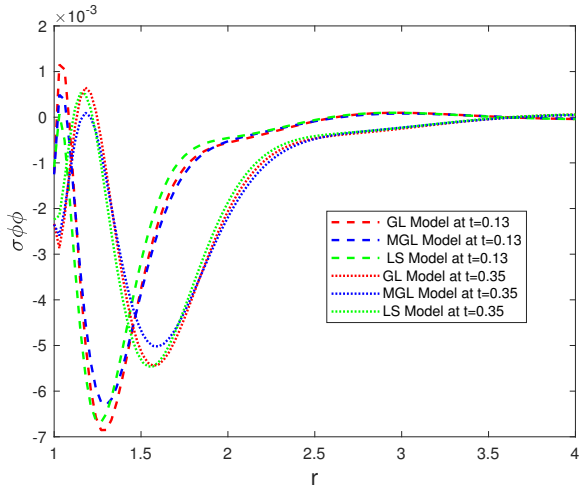

Figure 2.8.4: Variation of hoop stress for three models at time $t = 0.13$ and $t = 0.35$

From figures (2.8.3-2.8.4), it is evident that the radial stress and hoop stress exhibited by the LS model exhibit a notable deviation when compared to the GL and MGL models across all time intervals. At time $t = 0.13$, the stress components exhibit a notable increase followed by a rapid decrease as the radial distance increases. Eventually, the stress components converge towards zero.

Based on the analysis of figures (2.8.2-2.8.4), it is evident that there exists a notable variation in the predictions generated by various models in the vicinity of the cavity boundary, even at relatively small time intervals. Furthermore, this disparity becomes more pronounced for larger time value This is because the thermoelastic disturbance originates from the cavity's border.

2.9 Conclusion

This study focuses on the mathematical investigation of the recently suggested thermoelastic model known as the modified Green-Lindsay (MGL) model. The newly proposed model integrates strain and temperature rate factors into the constitutive equations, addressing the issue of discontinuity in displacement field that has been noticed by researchers in the context of the GL model. The current investigation focuses on the thermal shock phenomenon in an unbounded medium containing a cylindrical cavity. We demonstrate that the short-term approximated analytical solutions for various field variables in the MGL model can be expressed as a combination of a wave component and a diffusive component. Notably, the diffusive component propagates at an infinite speed, similar to what is observed in classical thermoelasticity theory. In addition, we proceed to address the issue using numerical methods and demonstrate a notable variance between the estimates generated by this particular model and other generalized models such as LS and GL models in close proximity to the cavity border at a low time value. Moreover, the difference becomes more pronounced as the time value grows. The

MGL model exhibits a greater domain of effect for the field variables in comparison to other models.